ISSN 1674-1056
http://cpb.iphy.ac.cn
http://iopscience.iop.org/cpb
中国物理 B
Chinese Physics
中国物理 Chinese Physics B

Hunting down the ohmic contact of organic field-effect transistor

M Micjan, M Novota, P Telek, M Donoval, M Weis
Citation: Chin. Phys. B . 2019, 28(11): 118501 . **doi:** 10.1088/1674-1056/ab44a1
Journal homepage: http://cpb.iphy.ac.cn; http://iopscience.iop.org/cpb

What follows is a list of articles you may be interested in

Performance improvement of 4H-SiC PIN ultraviolet avalanche photodiodes with different intrinsic layer thicknesses

Xiaolong Cai(蔡小龙), Dong Zhou(周东), Liang Cheng(程亮), Fangfang Ren(任芳芳), Hong Zhong(钟宏), Rong Zhang(张荣), Youdou Zheng(郑有炓), Hai Lu(陆海)
Chin. Phys. B . 2019, 28(9): 098503 . **doi:** 10.1088/1674-1056/ab343f

Effects of hole-injection through side-walls of large V-pits on efficiency droop in Ⅲ-nitride LEDs

Dong-Yan Zhang(张东炎), Jie Zhang(张洁), Xiao-Feng Liu(刘晓峰), Sha-Sha Chen(陈沙沙), Hui-Wen Li(李慧文), Ming-Qing Liu(刘明庆), Da-Qian Ye(叶大千), Du-Xiang Wang(王笃祥)
Chin. Phys. B . 2019, 28(4): 048501 . **doi:** 10.1088/1674-1056/28/4/048501

Bright hybrid white light-emitting quantum dot device with direct charge injection into quantum dot

Jin Cao(曹进), Jing-Wei Xie(谢婧薇), Xiang Wei(魏翔), Jie Zhou(周洁), Chao-Ping Chen(陈超平), Zi-Xing Wang(王子兴), Chulgyu Jhun(田哲圭)
Chin. Phys. B . 2016, 25(12): 128502 . **doi:** 10.1088/1674-1056/25/12/128502

Introduction of F_4-TCNQ/MoO_3 layers for thermoelectric devices based on pentacene

Wu Shuang-Hong, Ryosuke Nakamichi, Masatsugu Taneda, Zhang Qi-Sheng, Chihaya Adachi
Chin. Phys. B . 2014, 23(9): 098502 . **doi:** 10.1088/1674-1056/23/9/098502

A high mobility C_{60} field-effect transistor with an ultrathin pentacene passivation layer and bathophenanthroline/metal bilayer electrodes

Zhou Jian-Lin,Yu Jun-Sheng,Yu Xin-Ge,Cai Xin-Yang
Chin. Phys. B . 2012, 21(2): 027305 . **doi:** 10.1088/1674-1056/21/2/027305

Hunting down the ohmic contact of organic field-effect transistor*

M Micjan, M Novota, P Telek, M Donoval, and M Weis†

Institute of Electronics and Photonics, Slovak University of Technology, Ilkovičova 3, Bratislava 81219, Slovakia

(Received 10 July 2019; revised manuscript received 29 August 2019; published online 18 October 2019)

We report properties of contact resistances observed on pentacene organic field-effect transistors (OFET) with four different source/drain electrodes, namely, copper (Cu), gold (Au), silver (Ag), and germanium (Ge). The metals were selected to provide a wide range of energy barriers for charge injection, from blocking contact to smooth injection. All OFETs exhibited strong voltage dependence of the contact resistance, even for devices with smooth injection, which is in strong disagreement with the definition of ohmic contacts. A comparison with current crowding, resistive network, Fowler–Nordheim tunneling, and electric field enhanced thermionic injection (Schottky emission) pointed to importance of local electric fields and/or electrostatic field charges.

Keywords: organic field-effect transistors, contact resistance, charge injection

PACS: 85.30.–z, 73.40.Cg, 73.61.Ph **DOI:** 10.1088/1674-1056/ab44a1

1. Introduction

Since the first organic field-effect transistor (OFET) was successfully demonstrated in the 1980s,[1,2] OFET devices have been used for the fundamental study of charge behavior in organic semiconductors, and also for promising applications. In the last three decades, a huge amount of progress in organic semiconductor synthesis has brought novel materials with properties such as air stability, low-cost synthesis, solubility, and high charge mobility. Meanwhile, device physics and electronics research has mostly concentrated on the fabrication technology, downscaling of devices to reach high device density, high output current, and fast switching speed.[3–5]

As the channel length becomes shorter, the charge transport through the device is even more affected by the injection properties and the electrode–organic semiconductor interface has become increasingly important. In other words, the short-channel devices exhibit significantly lower effective mobility due to potential drop on the injection electrode. The charge behavior on the electrode–organic semiconductor interface has been identified as a bottleneck of advanced OFET devices and an investigation of the underlaying physics has been envisioned as essential to obtain smooth injection.[6–14] The potential drop on an injection electrode is usually represented by the contact resistance as an important figure of merit for contacts. In addition, the contact resistance, which is an element of electrical equivalent circuit, is also a powerful tool for circuit design and modeling.[15,16] However, it has a deep physical meaning and many possible origins of the energy barrier have been proposed, such as energy level mismatch between the Fermi level of the injection electrode and the highest occupied molecular orbital (HOMO) level of an organic semiconductor with p-type conductivity, interfacial energy states, interfacial dipoles, mirror charge, internal electric field generated by traps, and so on.[17,18] Furthermore, the contact resistance has been found to be affected by many parameters, such as the gate insulator,[19] metal deposition rate of the injection electrodes,[20–22] injection electrode geometry,[23,24] or charge transport through channel.[25]

The charge injection on metal–semiconductor interface is a complex problem. There are a couple of charge injection processes that can take place, such as direct tunneling, Fowler–Nordheim tunneling, hopping through interfacial states, or electric-field enhanced thermionic emission (i.e., the Schottky effect).[6,26] The physics of inorganic semiconductor devices in accordance to the charge injection recognizes two fundamental kinds of contacts: (i) Schottky contacts and (ii) ohmic contacts.[27] The Schottky contacts provide rectifying behavior, often exhibit high contact resistance, and the charge injection is ruled by the electric-field enhanced thermionic emission. The requirement for ohmic contacts with low contact resistance is a common reduction of the definition because the most important property of ohmic contacts is their non-rectifying behavior (i.e., linear current–voltage, I–V, dependence). Consequently, the ohmic nature of contacts of OFET devices has often been verified by the linearity of the output current characteristics in low-voltage region.[28–31] However, the definition of the ohmic contacts through the contact resistance R_c as

$$R_c = \frac{\partial V}{\partial I} = \text{const.} \tag{1}$$

has not been established for three-terminal devices, such as transistors. Hence, a more detailed analysis of the contact re-

*Project supported by the Slovak Research and Development Agency (Grant Nos. APVV-17-0501 and APVV-17-0522) and the Slovak Grant Agency for Science (Grants No. 1/0776/15).

†Corresponding author. E-mail: martin.weis@stuba.sk

© 2019 Chinese Physical Society and IOP Publishing Ltd

sistance is required to confirm if the ohmic contact has been achieved.

The present work is focused on OFET devices with pentacene as an organic semiconductor and several metals are used for source/drain contacts. The contact resistance is evaluated by the transmission line method (TLM) for various gate–source voltages and the voltage dependence is analyzed. We show that the metals that are generally assumed to be suitable for ohmic contacts of pentacene OFETs provide low contact resistance but not ohmic behavior. In addition, the voltage dependence is compared with several microscopic and macroscopic models to find the most suitable explanation.

2. Experimental details

In this study, OFET devices with top-contact bottom-gate geometry were fabricated using silicon wafers with 110 nm thermally grown silicon dioxide (SiO_2) layer as the substrates. The substrates were cleaned in an ultrasonic bath subsequently by 20 vol.% ethanolamine aqueous solution, acetone, isopropyl alcohol, and in deionized water prior to further processing. Poly(methyl methacrylate) (PMMA, Sigma-Aldrich) was dissolved in toluene (Sigma-Aldrich) with a concentration of 3 wt.%. The PMMA solution was sonicated for 30 min and subsequently filtered through 0.22 μm sized polytetra fluoroethylene (PTFE) filter to remove insoluble particles. The solutions of PMMA were spun on to the substrates at 3000 rpm for 30 s and the prepared films were subsequently annealed at 160 °C for 90 min in ambient atmosphere to remove residual solvent prior the deposition of semiconducting layer. The PMMA film thickness estimated by Dektak 150 (Bruker, USA) mechanical profilometer was 70 nm. Consequently, the heavily-doped conductive Si wafers served as a gate electrode, whereas a gate dielectric layer was the PMMA/SiO_2 bilayer. Then, a 100 nm-thick pentacene layer was thermally evaporated in vacuum with pressure lower than 10^{-4} Pa with fixed deposition rate of 2.4 nm/min. After the deposition of the semiconducting pentacene layer, selected metal was thermally evaporated through the shadow mask to form source and drain electrodes. Here, we used four different metals (Au, Ag, Cu, Ge) for the source/drain electrodes. The OFET devices had channel lengths L and width W of 50–200 μm and 2.5 mm, respectively. The structure of the fabricated OFETs is depicted in Fig. 1(a). The transfer and output characteristics of the OFET devices have been recorded under ambient atmosphere using a Keysight B1500A semiconductor parameter analyzer (Keysight, USA).

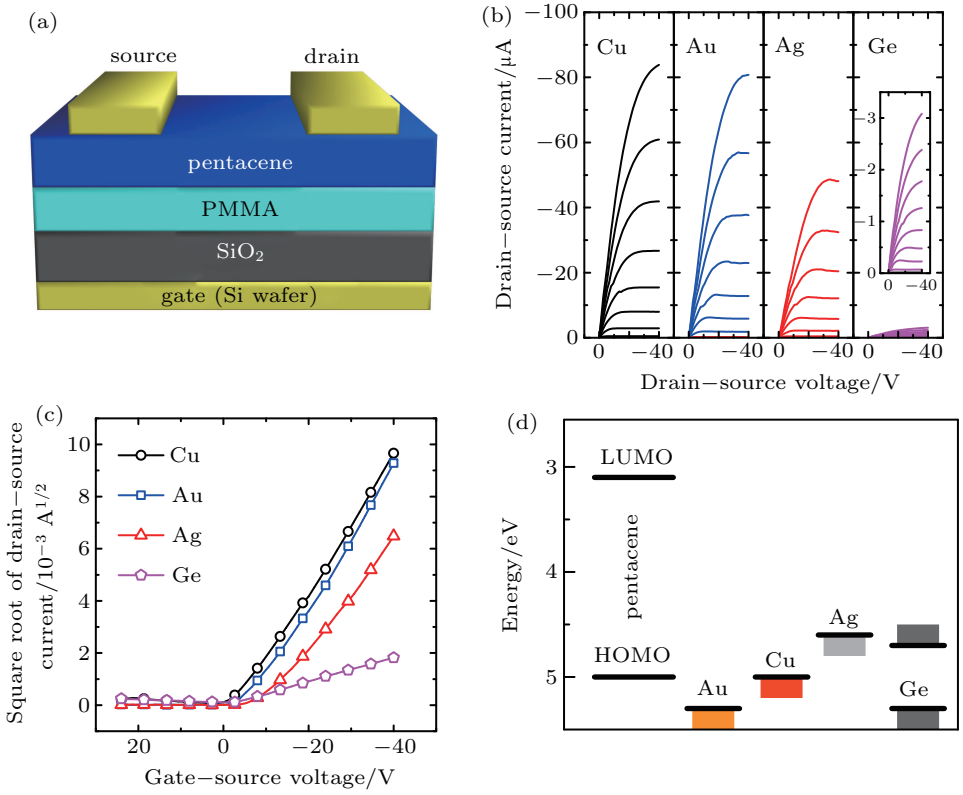


Fig. 1. (a) Sketch of fabricated OFET device, and (b) output and (c) transfer characteristics of the OFET devices using various metals for source/drain electrodes. (d) Energy band diagram of pentacene and the materials applied for injection electrodes.

3. Results and discussion

The output and transfer characteristics of the fabricated devices with four different injection electrode metals are presented in Figs. 1(b) and 1(c). Even though all devices exhibit transistor behavior, the drain–source currents differ for various injection electrodes. It should be mentioned here that the

energy mismatch between the highest occupied molecular orbital (HOMO) of the hole-conductivity organic semiconductor and the Fermi energy of the electrode is recognized as an injection barrier. Figure 1(d) illustrates the energy band diagram of pentacene and the materials applied for injection electrodes. Holes are transported in pentacene at the HOMO level of 5.0 eV, while Au, Cu, Ag, and Ge have the Fermi energy levels at 5.3 eV, 5.0 eV, 4.6 eV, and 5.0 eV, respectively.[32] Note that Ge is a semimetal with the energy gap of 0.67 eV at the room temperature. The selected materials provide a wide range of energy barriers that can be used for study of the injection through the interface between the electrode and organic semiconductor. In accordance to IEEE 1620 standards,[33] the field-effect mobility is estimated from the saturation region where the drain–source voltage V_{ds} is considerably larger than the gate–source voltage V_{gs} reduced by the threshold voltage V_{th}. Hence, the drain–source current I_{ds} in the saturated region of transfer characteristics in accordance to the gradual channel approximation model follows the relation

$$I_{ds} = \frac{WC_g\mu_{eff}}{2L}(V_{gs} - V_{th})^2, \tag{2}$$

where C_g is the gate insulator capacitance per unit of area and μ_{eff} is the effective field-effect mobility. It should be noted here that even though the effective mobility stands for charge transport properties through the organic semiconductor, it is affected by other processes, e.g., charge trapping in the organic semiconductor or insufficient injection from the source electrode. The devices with various metals used for electrodes exhibited the effective mobilities that are listed in Table 1.

Table 1. List of mobility values of of OFET devices using various metals for source/drain electrodes. The effective value was extracted by Eq. (2), whereas the contact-resistance-free value was estimated at −40 V by Eq. (3). Errors represent the standard deviation through a group of devices measured in the saturation region or fitting uncertainty of the TLM model.

Metal	Mobility/cm^2·V^{-1}·s^{-1}	
	Effective value	Contact-resistance-free value
Cu	0.20 ± 0.02	0.22 ± 0.02
Au	0.19 ± 0.01	0.22 ± 0.01
Ag	0.16 ± 0.02	0.21 ± 0.02
Ge	0.010 ± 0.004	0.19 ± 0.09

Given that the devices differ by the injection electrode only, the different effective mobilities should obviously originate in the injection barrier at the metal–organic semiconductor interface. Cu and Au are well known for smooth hole injection to pentacene, whereas Ag was reported to have a considerable energy barrier for holes.[34–36] Obviously, the device with Ge electrodes exhibits significantly lower effective mobility. Since the effective mobility is evaluated for an ideal OFET with smooth injection, the suppression of the effective mobility represents the effect of energy barrier on injected charge carriers. In other words, the contact resistance reduces the effective mobility. Meanwhile, the output characteristics in linear region (i.e., $|V_{ds}| \ll |V_{gs} - V_{th}|$) show a linear relationship between the applied voltage and output current for all injection electrodes, see Fig. 2; hence, the contacts exhibit ohmic-like behavior. Because low resistance is not a requirement for ohmic contacts, we should not denote it as the Schottky only because of higher resistance value.

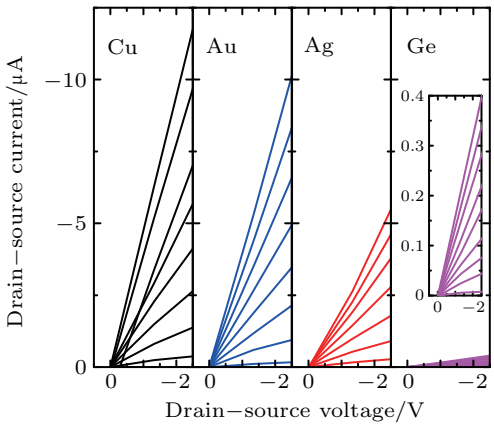


Fig. 2. Detailed view of output characteristics linear region of the OFET devices using various metals for source/drain electrodes. The output characteristics were recorded for the gate–source voltage varied from 0 to −40 V (step 5 V).

The ohmic contact as defined by Eq. (1) needs to be evaluated for the metal–organic semiconductor interface only; thus, the linearity of the output characteristics in linear region may be misleading evaluation. The contact resistance can be evaluated by various approaches, such as transmission line method,[37,38] gated 4-probe measurement,[39] or Y-function method.[40] The TLM is a popular model to evaluate the contact resistance as superposition of the channel resistance R_{ch} and the contact resistance. Thus, if an OFET device is working in linear regions, then the total device resistance R_{tot} follows the relation

$$R_{tot} = R_c + R_{ch} = R_c + \frac{L}{WC_g\mu_0\left(V_{gs} - V_{th}\right)}, \tag{3}$$

where the channel resistance scales with channel length L and the contact resistance is a channel-length-independent parameter. Consequently, linear extrapolation of the total resistance to the zero channel length ($L = 0$) provides the contact resistance. The slope of the linear function is related to the channel transconductance and can be used for estimation of the "contact resistance-free" mobility μ_0. The TLM plots for the OFET devices with various injection electrode are depicted in Fig. 3. At first glance, the voltage dependence of the total resistance is clearly visible. Both injection and transport properties exhibit dependence on the applied gate–source voltage. It has been reported that the contact resistance and the mobility of OFET devices are voltage dependent parameters.[19,41,42] Obviously, even though the offset of the TLM plot deviates sig-

nificantly for any selected voltage, the slope is almost conserved. Consequently, the contact-resistance-free mobility of about 0.22 $cm^2/V{\cdot}s$ extracted from the TLM analysis illustrates almost identical charge transport through the organic semiconductor layer and the suppression of the effective mobility is caused by insufficient injection, see Table 1.

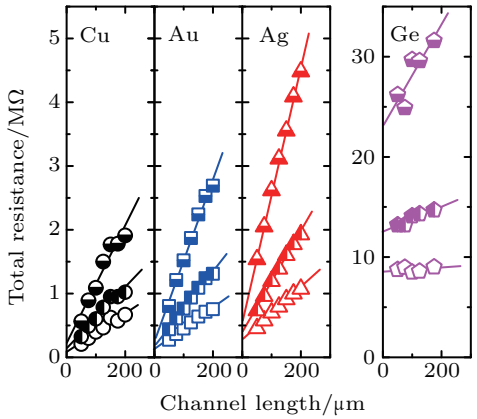


Fig. 3. Transmission-line method analysis of the OFET devices using various metals for source/drain electrodes under applied gate–source voltages of −20 V, −30 V, and −40 V.

Figure 4 illustrates the voltage dependence of the estimated contact resistances of the OFET devices using various metals for source/drain electrodes. Although the Cu and Au electrodes provide the lowest contact resistances, they also exhibit dependence on the applied gate–source voltage. Because ohmic contacts are defined by voltage independent contact resistance, these metals provide only low-resistance nonohmic contacts. In other words, the ohmic contacts are not formed, even though the contact resistance is significantly decreased in comparison with that of other metals. The voltage dependence of contact resistance reflects the underlaying physics; therefore, its detailed study is required. Various phenomena have been suggested for the voltage dependence of injection properties. The low-voltage low-temperature region is usually ruled by the direct tunneling. A rise of temperature supports the electric field-enhanced thermionic injection, while the increase of the applied electric field follows the Fowler–Nordheim tunneling. Meanwhile, the injection properties can also be affected by the charge transport properties. The macroscopic current density distribution is denoted as 'current crowding' and the distribution is modeled by the resistive network. The following part focuses on these phenomena and examine suitability for the voltage dependence of the organic transistor contact resistance.

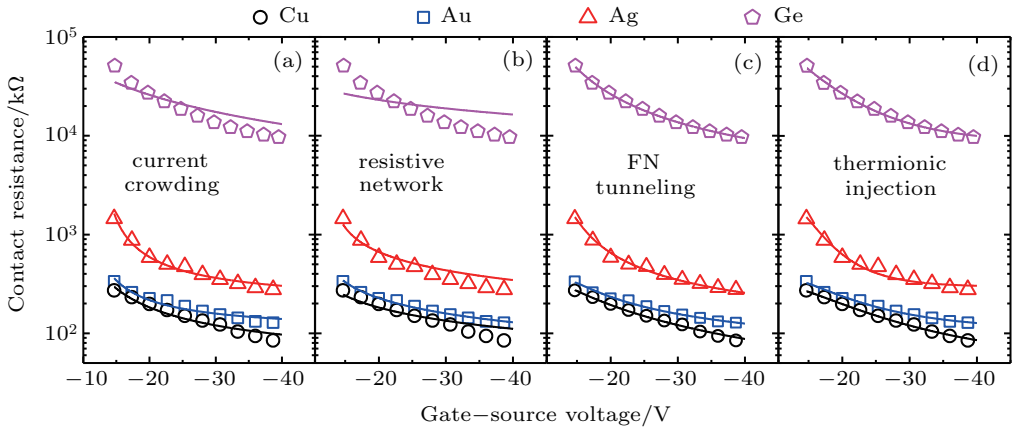


Fig. 4. Voltage dependence of observed contact resistance of the OFET devices using various metals for source/drain electrodes. Solid lines stand for various models ((a) current crowding, (b) resistive network, (c) Fowler–Nordheim tunneling, and (d) thermionic injection) of the contact resistance.

Current crowding in organic electronics is a well-accepted phenomenon in sandwich structures such as OLED devices,[43] it has also been suggested for OFET devices.[12] Although there is a huge overlap of the source and gate electrodes, in the steady state only the electrode's edge contributes to the charge injection. Hence, the injection process is a balance between the organic semiconductor resistance in the channel region and the metal contact resistivity. Consequently, the charge is injected from an effective area that is defined as a product of the channel width W and the transfer length L_T (the characteristic injection length).[12,23,44,45] The contact resistance in the current crowding model is ruled by the carrier concentration and follows[12]

$$R_{c,CC} = \frac{(\mu C)^{-1}}{V_{gs} - V_{th}} + R_{c,0}, \tag{4}$$

where $R_{c,0}$ is the voltage independent parasitic resistance and μC is the product of mobility μ and effective capacitance C. This model plays a role mostly in power devices with high current densities, where self-heating takes place. Although it is macroscopic model, it is based on the device physics and electrothermal properties.

Another macroscopic model is the resistive network[9] using circuit theory concepts, where we break the problem into small parts so that the circuit element dimensions will be infinitesimal small. In other words, the injection electrode re-

gion can be divided into infinitely small slices, and the contact resistance of each slice is represented by distributed parameters (units per unit of length). Subsequent integration leads to the contact resistance

$$R_{\mathrm{c,RN}} = \frac{1}{W}\sqrt{\frac{\rho_{\mathrm{c}}}{\mu C_{\mathrm{g}}(V_{\mathrm{gs}} - V_{\mathrm{th}})}} + R_{\mathrm{c},0}, \tag{5}$$

where ρ_{c} is the specific contact resistance dependent on the energy barrier of the metal/organic semiconductor interface. This model is applicable for large source/gate electrode area overlap and it has a capability to include the device geometry factors.

There are several microscopic models for the metal/organic semiconductor interface. However, direct tunneling will be not discussed in detail here because it is a voltage independent contact resistance and causes ohmic behavior of contacts. The so-called Fowler–Nordheim tunneling is common for applied voltages V higher than energy barrier height Φ_{B} ($V > \Phi_{\mathrm{B}}/e$, where e is the elementary charge) and is characterized by the current–voltage dependence

$$I \propto V^2 \exp\left(-\frac{4d\sqrt{2m}\Phi^{3/2}}{3e\hbar V}\right), \tag{6}$$

where d is the effective electrode separation, m is the effective electron mass, and $\hbar$ is the reduced Planck constant. Hence, the contact resistance in the OFET device follows the relation

$$R_{\mathrm{c,FN}} = \frac{R_0 V_0}{V_{\mathrm{gs}} - V_{\mathrm{th}} - 1/2}\exp\left(-\frac{V_0}{V_{\mathrm{gs}} - V_{\mathrm{th}}}\right) + R_{\mathrm{c},0}, \tag{7}$$

where R_0 and V_0 are fitting constants. It should be noted that even though Fowler–Nordheim tunneling has been proposed for OFET devices,[46] it is not a common model. The model is applicable for devices with high local electric fields that make the energy barriers more narrow.

The electric field-enhanced thermionic injection is also known as the Schottky emission. Briefly, the height of the potential barrier is lowered due to the combination of the applied electric field and the image force. The current through the metal/organic semiconductor interface is expressed by the thermionic emission (Schottky) current I_{Sch} enhanced by the electric field E as follows:

$$I = I_{\mathrm{Sch}} \exp\left(\frac{\beta\sqrt{E}}{kT}\right), \tag{8}$$

where $\beta = \sqrt{e^3/4\pi\varepsilon_0\varepsilon_{\mathrm{r}}}$ is the Schottky parameter and kT is the thermal energy (ε_0, ε_{r}, and k are the dielectric constant of vacuum, the relative dielectric constant of the organic semiconductor, and the Boltzmann constant, respectively). For a three-terminal structure, such as an OFET device, the contact resistance can be derived from the relation[47]

$$R_{\mathrm{c,Sch}} = R_{\mathrm{Sch}}\frac{(V_{\mathrm{gs}} - V_{\mathrm{th}})/V_{\mathrm{Sch}}}{\exp\left(\sqrt{(V_{\mathrm{gs}} - V_{\mathrm{th}})/V_{\mathrm{Sch}}}\right)} + R_{\mathrm{c},0}, \tag{9}$$

where R_{Sch} and V_{Sch} are the characteristic resistance and voltage, respectively. The characteristic resistance R_{Sch} is proportional to the zero-field energy barrier, whereas the characteristic voltage V_{Sch} is related to the electric-field coefficient β/kT. This model should be suitable for energy barriers lowered by the electric field.

Obviously, the macroscopic models such as current crowding and resistive network cannot follow the voltage dependence of the contact resistances sufficiently, whereas the microscopic levels are in good agreement with the experimental results. The precision of the fit is evaluated using the adjusted coefficient of determination as depicted in Fig. 5. There is no significant difference between the Fowler–Nordheim tunneling and electric field enhanced thermionic injection (Schottky emission) models. Interestingly, both microscopic models fit the experimental data for various energy barrier heights, as well as applied voltages. Even though this analysis does not allow us to distinguish between electric field driven tunneling and potential barrier lowering processes, both are caused by local electric fields and/or electrostatic field of charges (image charge). As a result, the energy barrier plays a key role for charge injection and causes the voltage dependence of the contact resistance. Hence, all materials provide so-called Schottky contacts even for low contact resistance. In other words, electrode materials such as Au and Cu provide lower contact resistance; however, we cannot denote them as the ohmic contacts.

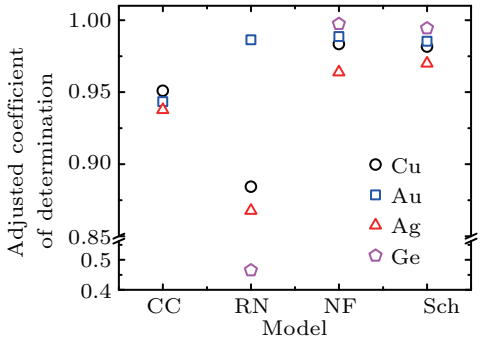


Fig. 5. Evaluated adjusted coefficient of determination for fittings shown in Fig. 4. The models are current crowding (CC), resistive network (RN), Fowler–Nordheim tunneling (FN), and thermionic injection also denoted as Schottky emission (Sch).

4. Conclusion

We have reported the voltage dependences of contact resistances observed on pentacene OFET devices with four different source/drain electrodes, namely, Cu, Au, Ag, and Ge. The metals selected for the electrodes provide a wide range of energy barriers for charge injection to give us a chance to investigate low and high contact resistances. All of the fabricated devices exhibited strong voltage dependence of the contact resistance, which is in disagreement with the definition of ohmic contacts. A detailed comparison with macro-

scopic and microscopic models for the voltage dependence of the contact resistance has revealed the possibility of Fowler–Nordheim tunneling and electric field enhanced thermionic injection (Schottky emission). Hence, even though we are able to reach relatively low contact resistance, there is no ohmic contact at all.

References

[1] Kudo K, Yamashina M and Moriizumi T 1984 *Jpn. J. Appl. Phys.* **23** 130
[2] Tsumura A, Koezuka H and Ando T 1986 *Appl. Phys. Lett.* **49** 1210
[3] Kumar B, Kaushik B K and Negi Y S 2014 *Polymer Reviews* **54** 33
[4] Fukuda K, Takeda Y, Yoshimura Y, Shiwaku R, Tran L T, Sekine T, Mizukami M, Kumaki D and Tokito S 2014 *Nat. Commun.* **5** 4147
[5] Weis M 2017 *Encyclopedia of Physical Organic Chemistry* (Wang Z, Ed.) (New York: John Wiley) p. 3565
[6] Liu C, Xu Y and Noh Y Y 2015 *Mater. Today* **18** 79
[7] Liu C, Huseynova G, Xu Y, Long D X, Park W T, Liu X, Minari Y and Noh Y Y 2016 *Sci. Rep.* **6** 29811
[8] Natali D and Caironi M 2012 *Adv. Mater.* **24** 1357
[9] Marinkovic M, Belaineh D, Wagner V and Knipp D 2012 *Adv. Mater.* **24** 4005
[10] Gruber M, Schürrer F and Zojer K 2012 *Org. Electron.* **13** 1887
[11] Wang S D, Yan Y and Tsukagoshi K 2010 *Appl. Phys. Lett.* **97** 063307
[12] Richards T J and Sirringhaus H 2007 *J. Appl. Phys.* **102** 094510
[13] Gundlach D J, Zhou L, Nichols J A, Jackson T N, Necliudov P V and Shur M S 2006 *J. Appl. Phys.* **100** 024509
[14] Minari T, Miyadera T, Tsukagoshi K and Aoyagi T 2007 *Appl. Phys. Lett.* **91** 053508
[15] Kim C H, Bonnassieux Y and Horowitz G 2014 *IEEE T. Electron Dev.* **61** 278
[16] Tejada J A J, Villanueva J A L, Varo P L, Awawdeh K M and Deen M J 2014 *IEEE T. Electron Dev.* **61** 266
[17] Koch N, Kahn A, Ghijsen J, Pireaux J J, Schwartz J, Johnson R L and Elschner A 2003 *Appl. Phys. Lett.* **82** 70
[18] Ishii H, Sugiyama K, Ito E and Seki K 1999 *Adv. Mater.* **11** 605
[19] Blanchet G B, Fincher C R, Lefenfeld M and Rogers J A 2004 *Appl. Phys. Lett.* **84** 296
[20] Park J, Kang J M, Kim D W and Choi J S 2010 *Thin Solid Films* **518** 6232
[21] Xu Y, Liu C, Sun H, Balestra F, Ghibaudo G, Sheideler W and Noh Y Y 2014 *Org. Electron.* **15** 1738
[22] Cho J H, Kim D H, Jang Y, Lee W H, Ihm K, Han J H, Chung S and Cho K 2006 *Appl. Phys. Lett.* **89** 132101
[23] Xu Y, Liu C, Scheideler W, Darmawan P, Li S, Balestra F, Ghibaudo G and Tsukagoshi K 2013 *Org. Electron.* **14** 1798
[24] Gruber M, Zojer E, Schürrer F and Zojer K 2013 *Adv. Funct. Mater.* **23** 2941
[25] Xu Y, Liu C, Minari T, Darmawan P, Balestra F, Ghibaudo G and Tsukagoshi K 2013 *J. Appl. Phys.* **113** 064507
[26] Wang W, Lee T and Reed M A 2003 *Phys. Rev. B* **68** 035416
[27] Sze S M 1981 *Physics of Semiconductor Devices* (2nd Edn.) (New York: Wiley) p. 304
[28] Kao K C 2004 *Dielectric phenomena in solids: with emphasis on physical concepts of electronic processes* (Amsterdam: Elsevier) p. 327
[29] Di C, Wei D, Yu G, Liu Y, Guo Y and Zhu D 2008 *Adv. Mater.* **20** 3289
[30] Dinelli F, Murgia M, Biscarini F and De Leeuw D M 2004 *Synth. Met.* **146** 373
[31] Wu Y, Li Y and Ong B S 2006 *J. Am. Chem. Soc.* **128** 4202
[32] Haynes W M 2014 *CRC handbook of chemistry and physics* (New York: CRC press)
[33] Gamota D and Brazis P 2008 *J. IEEE Std.* **1620–2008** 1
[34] Diao L, Frisbie C D, Schroepfer D D and Ruden P P 2007 *J. Appl. Phys.* **101** 014510
[35] Jaeckel B, Sambur J B and Parkinson B A 2008 *J. Appl. Phys.* **103** 063719
[36] Wang S D, Minari T, Miyadera T, Tsukagoshi K and Aoyagi Y 2007 *Appl. Phys. Lett.* **91** 203508
[37] Necliudov P V, Shur M S, Gundlach D J and Jackson T N 2002 *Solid-State Electron.* **47** 259
[38] Klauk H, Schmid G, Radlik W, Weber W, Zhou L, Sheraw C D, Nichols J A and Jackson T N 2002 *Solid-State Electron.* **47** 297
[39] Pesavento P V, Chesterfield R J, Newman C R and Frisbie C D 2004 *J. Appl. Phys.* **96** 7312
[40] Xu Y, Minari T, Tsukagoshi K, Chroboczek J A and Ghibaudo G 2010 *J. Appl. Phys.* **107** 114507
[41] Minari T, Nemoto T and Isoda S 2006 *J. Appl. Phys.* **99** 034506
[42] Reese C and Bao Z 2009 *Adv. Funct. Mater.* **19** 763
[43] Park J W, Shin D C and Park S H 2011 *Semicond. Sci. Technol.* **26** 034002
[44] Wang H, Wang W, Sun P, Ma X, Li L, Liu M and Hao Y 2015 *IEEE Electron Dev. Lett.* **36** 609
[45] Wang H, Wang W, Sun P, Ma X, Li L, Liu M and Hao Y 2014 *Appl. Phys. Lett.* **104** 013301
[46] Schroeder R, Majewski L A and Grell M 2003 *Appl. Phys. Lett.* **83** 3201
[47] Li J, Ou-Yang W and Weis M 2017 *J. Phys. D: Appl. Phys.* **50** 035101